Design, Construction, and Utilization of the World's First Superconducting Linear Accelerator

Todd I Smith
Hansen Experimental Physics Labs
Stanford University

	Mark III	SC Linac
Energy	*1 GeV*	*2 GeV*
Voltage Gradient	*13 MV/m*	*14 MV/m*
Duty Factor	*5×10^{-4}*	*CW*
1.8 K cooling needed with $Q = 4 \times 10^{9}$	*n/a*	*7 kW*
Energy resolution	*10^{-2}*	*10^{-4}*
Average current	*<10 μA*	*100 μA*

Design, Construction, and Utilization of the World's First Superconducting Linear Accelerator

Todd I Smith
Hansen Experimental Physics Labs
Stanford University

	Mark III	SC Linac
Energy	*1 GeV*	*2 GeV*
Voltage Gradient	*13 MV/m*	*14 MV/m (one pass)* *2.8 MV/m (five passes)*
Duty Factor	*5×10^{-4}*	*CW*
1.8 K cooling needed with $Q = 4 \times 10^{9}$	*n/a*	*7 kW (one pass)* *280 W (five passes)*
Energy resolution	*10^{-2}*	*10^{-4}*
Average current	*<10 μA*	*100 μA*

Topics to be Covered

1. *Choice of accelerator structure for the superconducting linac (SCA)*
2. *Description and performance of the linac injector*
3. *Single pass regenerative beam breakup*
4. *Description and performance of the linac in NP experiments*
5. *Multipass regenerative beam breakup*
6. *Description and performance of the recyclotron in NP experiments*
7. *The linac and modified recyclotron in FEL experiments and in the demonstration of same-cell electron beam energy recovery.*

Choice of accelerator structure

Constraints: frequency=1.3 GHz; Length~6m (consistent with 14MeV/m, a 100μA beam and a 10 kW klystron/structure)

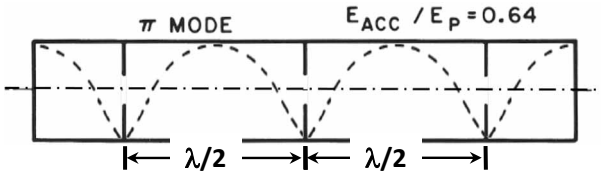

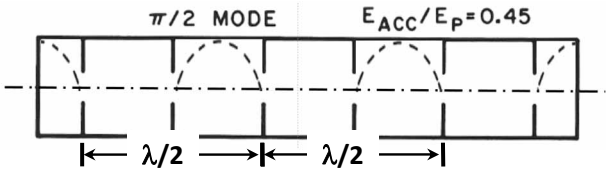

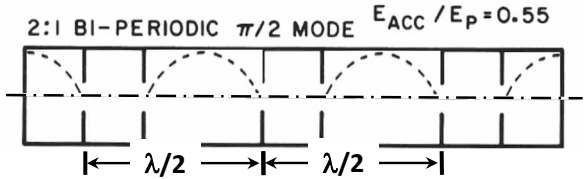

- *Chain of N coupled pillbox cavities has N normal modes*
- *Pi mode is "obviously" the most efficient*
- *In the 60s very competent accelerator physicists were adamant that the π mode wouldn't work and many argued passionately for the π/2 mode. Why?*
- *Nearly everything follows from the fact that* **any** *energy losses in the cavities require the eigenfrequencies of the normal modes to be complex and thus a pure mode cannot be excited.*
- *The excitation of unwanted modes is small as long as the relative frequency spacing between the desired mode and its nearest neighbor ($\Delta\omega/\omega$) is >>1/2Q.*
- *This leads to* $N_{\pi}^{2} \ll \frac{\pi^{2}\gamma}{4} Q$ *and* $N_{\pi/2} \ll \frac{\pi\gamma}{2} Q$.

- *The π mode is much less tolerant of fabrication errors than the π/2 mode, but still OK for SRF.*
- *Lack of unexcited cavities in the π mode convinced us to concentrate on a bi-periodic π/2 mode structure.*

Dispersion curve for 1.3 GHz center-fed 26 wavelength structure with coupling constant (γ)=1%.

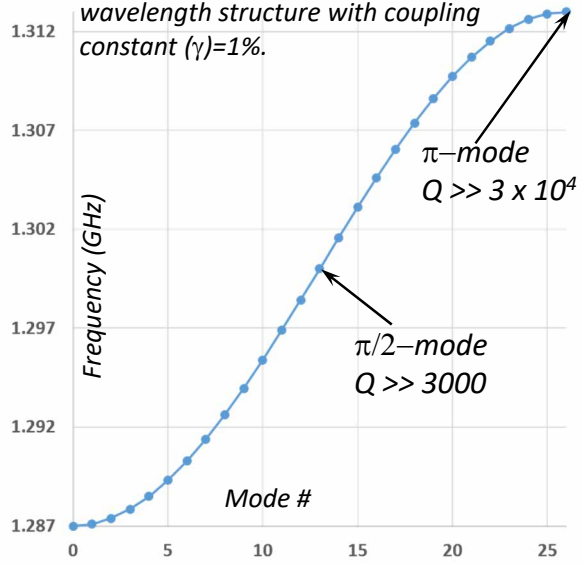

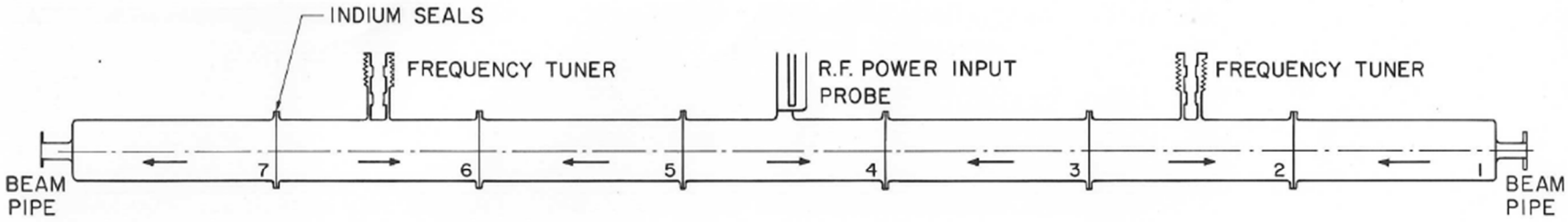

6 m ACCELERATOR STRUCTURE COMPOSED OF SEVEN 7/2 λ SUBSTRUCTURES

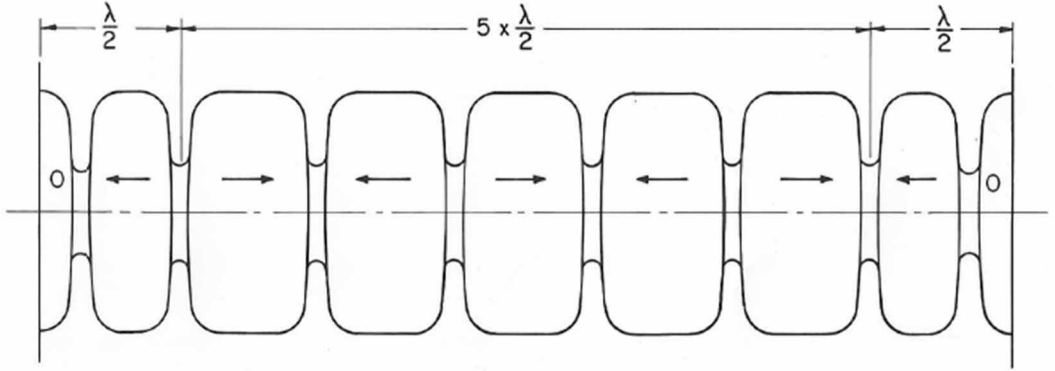

TYPICAL 7/2 λ SUBSTRUCTURE

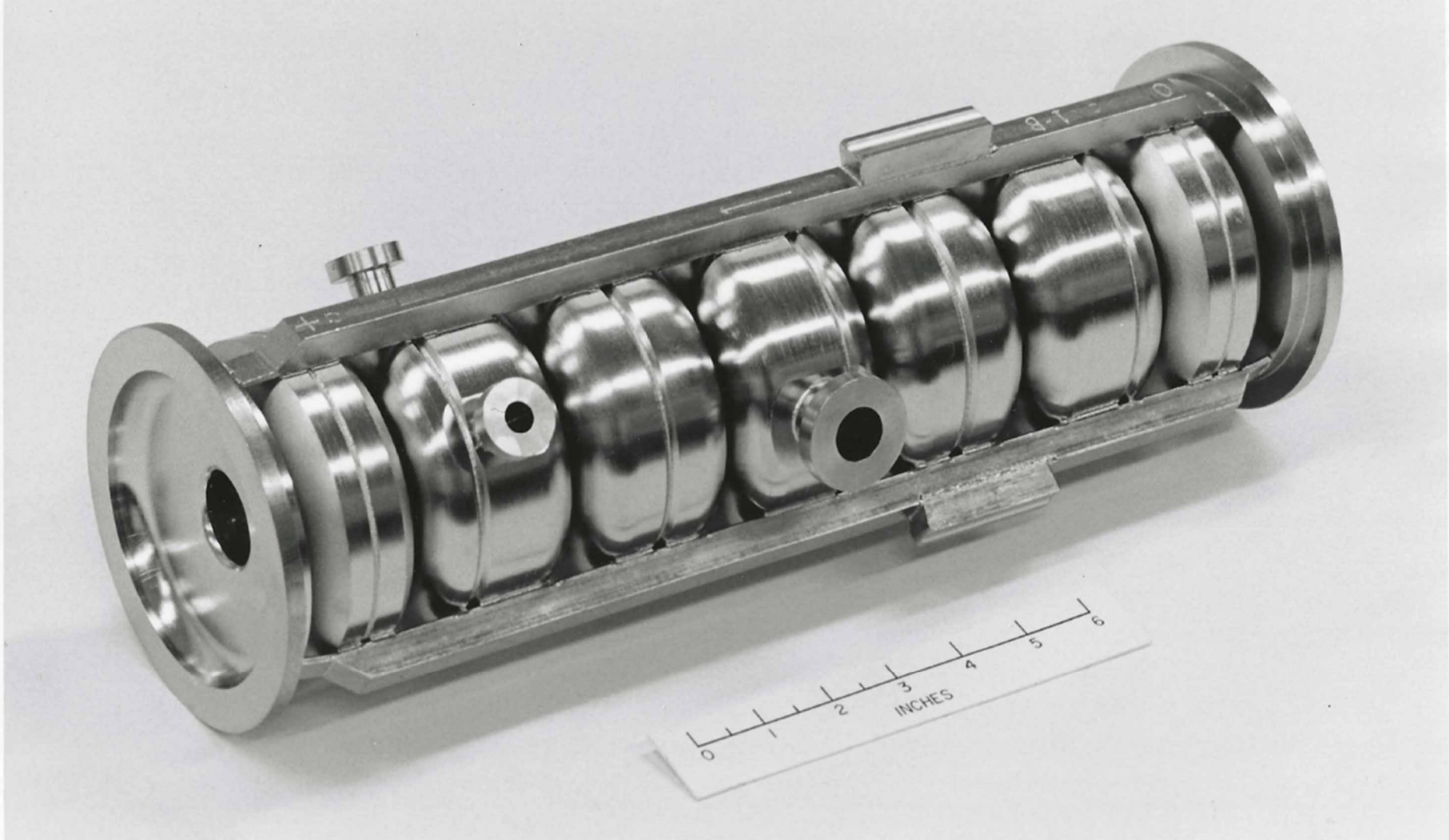
0
1
2
3
4
5
6
INCHES

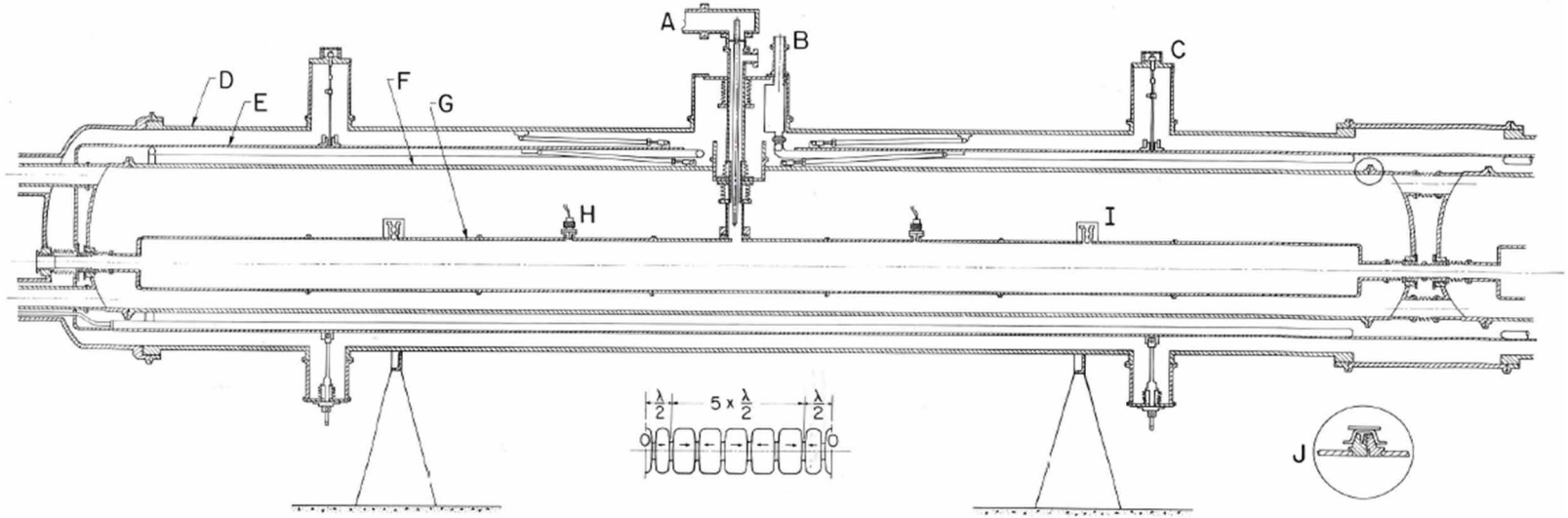

Assembled 20-foot accelerator dewar module. This section has end caps at one end and is connected to another module at the other end.

A. RF power input.
B. Liquid nitrogen vent.
C. Dewar support and alignment adjustment.
D. Vacuum jacket (36 in. diameter tank).
E. Liquid nitrogen shield.
F. Helium dewar (24 in. diameter tank).
G. Accelerator structure. This is assembled from seven units, one of which is detailed at bottom center.
H. Field sampling probe. (Output to feedback electronics.)
I. Structure tuner.
J. Detail of 24 in. diameter V-band indium seal.

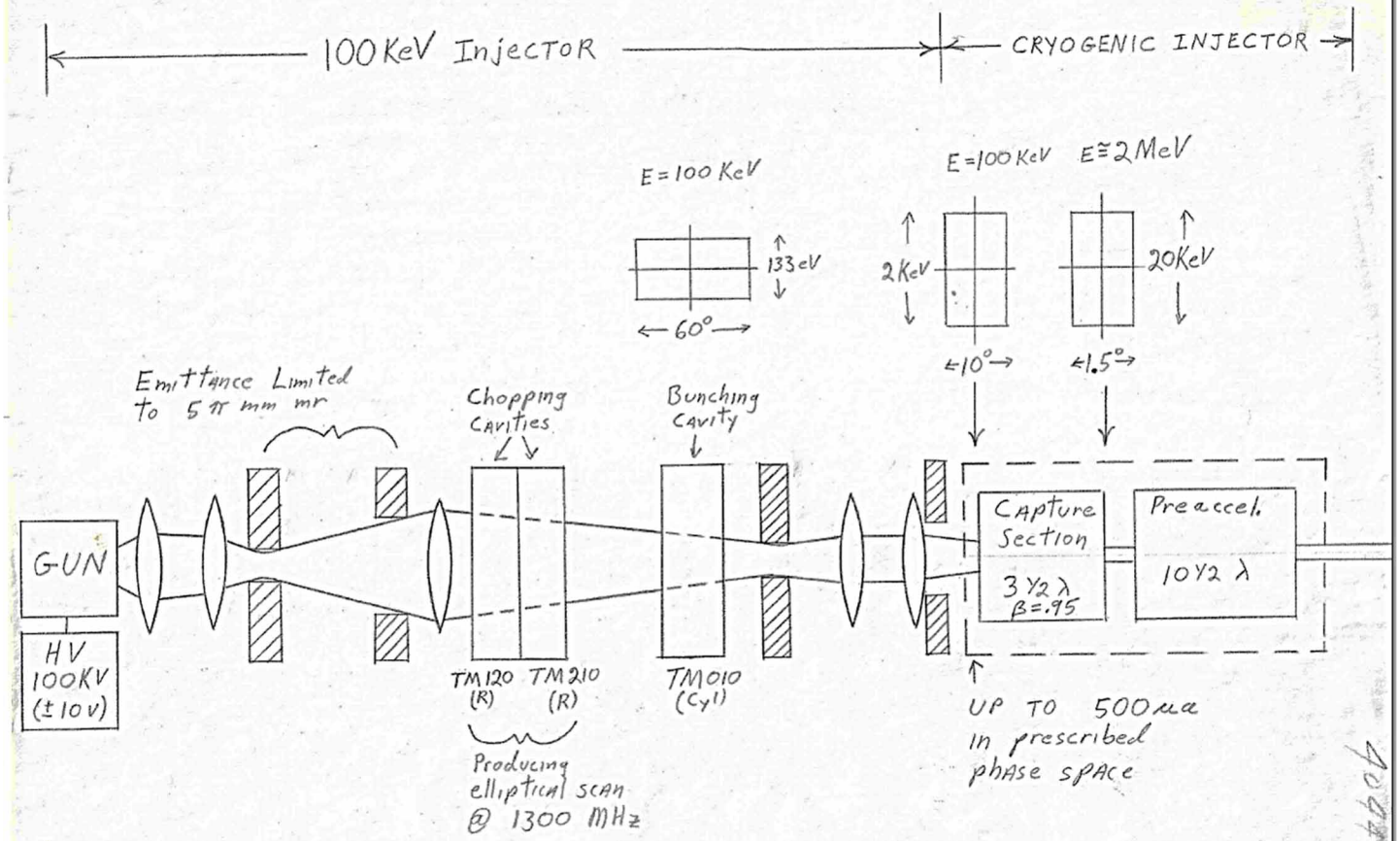
100 KeV Injector
CRYOGENIC INJECTOR
E = 100 KeV
133 eV
60°
E = 100 KeV
E ≅ 2 MeV
2 KeV
20 KeV
10°
1.5°
Emittance Limited to 5π mm mr
Chopping Cavities
Bunching Cavity
GUN
HV 100KV (± 10V)
TM120 (R)
TM210 (R)
TM010 (Cyl)
Capture Section
3 ½ λ β=.95
Preaccel.
10 ½ λ
UP TO 500 μa in prescribed phase space
Producing elliptical scan @ 1300 MHz
TS 3/23/77

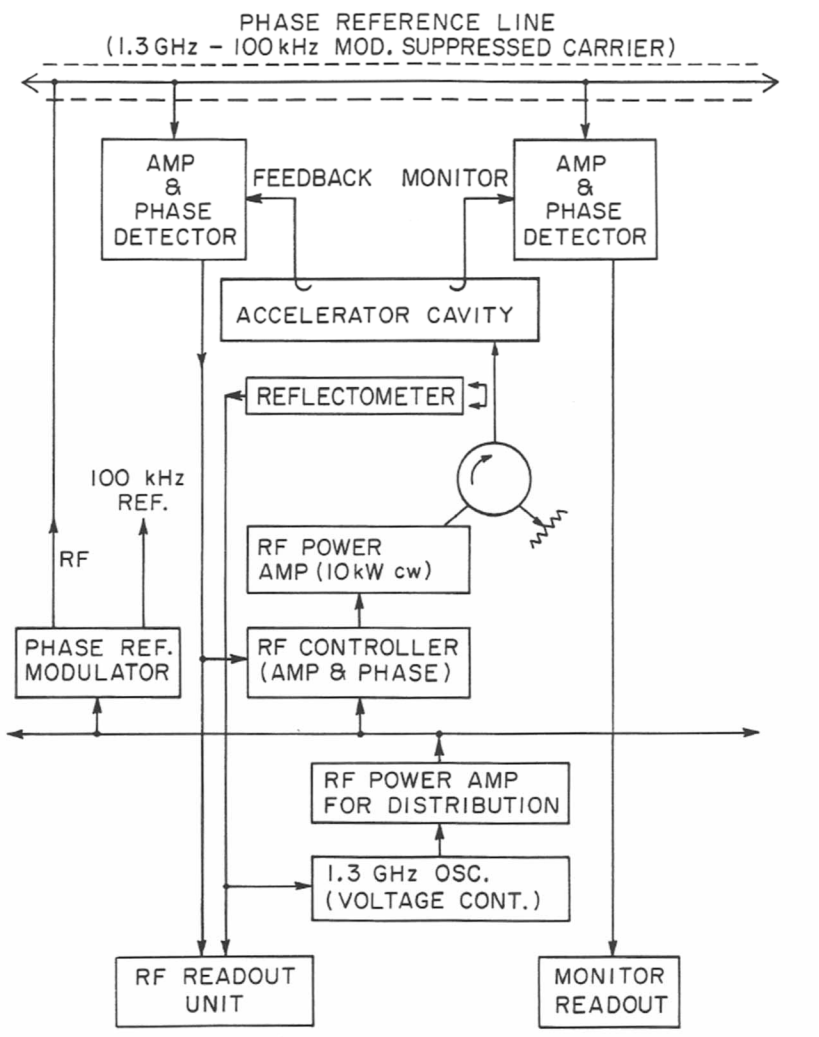
PHASE REFERENCE LINE
(1.3 GHz - 100 kHz MOD. SUPPRESSED CARRIER)
AMP & PHASE DETECTOR
FEEDBACK
MONITOR
AMP & PHASE DETECTOR
ACCELERATOR CAVITY
REFLECTOMETER
100 kHz REF.
RF
RF POWER AMP (10 kW cw)
PHASE REF. MODULATOR
RF CONTROLLER (AMP & PHASE)
RF POWER AMP FOR DISTRIBUTION
1.3 GHz OSC. (VOLTAGE CONT.)
RF READOUT UNIT
MONITOR READOUT

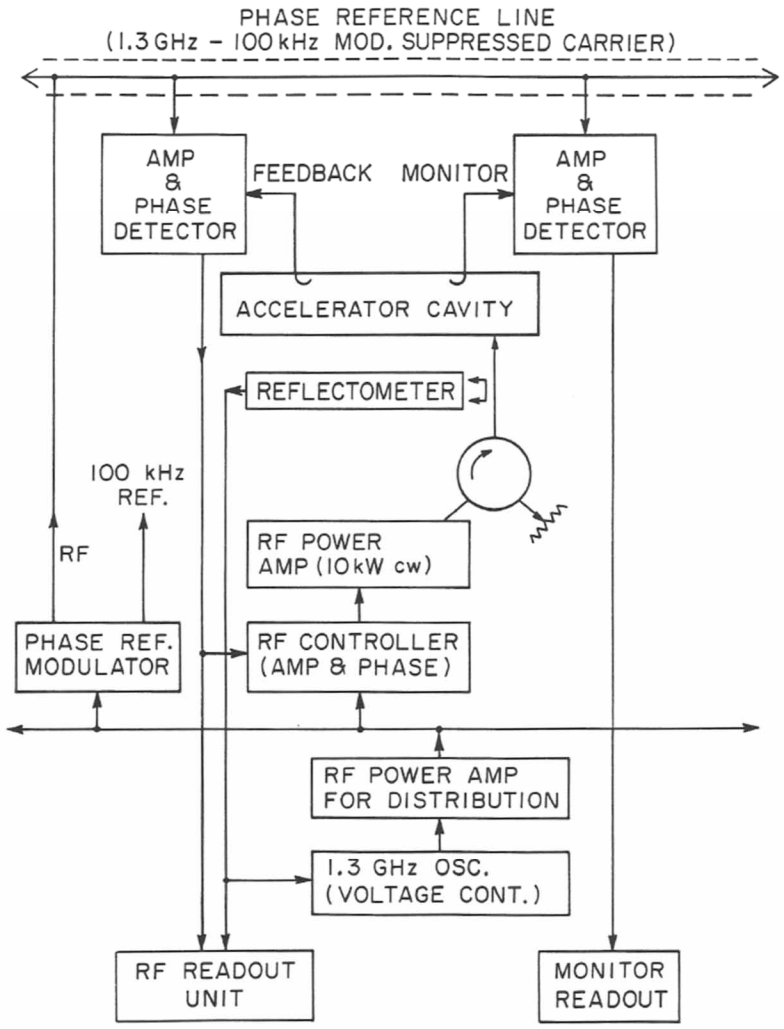

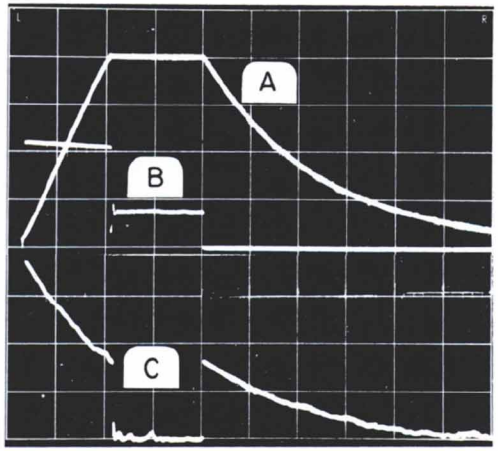

Oscilloscope traces obtained during a recent test with a pulsed reference voltage on a superconducting cavity structure. Trace (A) is the cavity voltage, trace (B) is the square root of the incident power (linear detectors), and trace (C) is the square root of the reflected power from the cavity structure. The time scale is 5 msec per division.

Demonstration of the superconducting electron accelerator as a high-intensity high-resolution device

M.S. McAshan, K. Mittag, H.A. Schwettman, L.R. Suelzle, and J.P. Turneaure

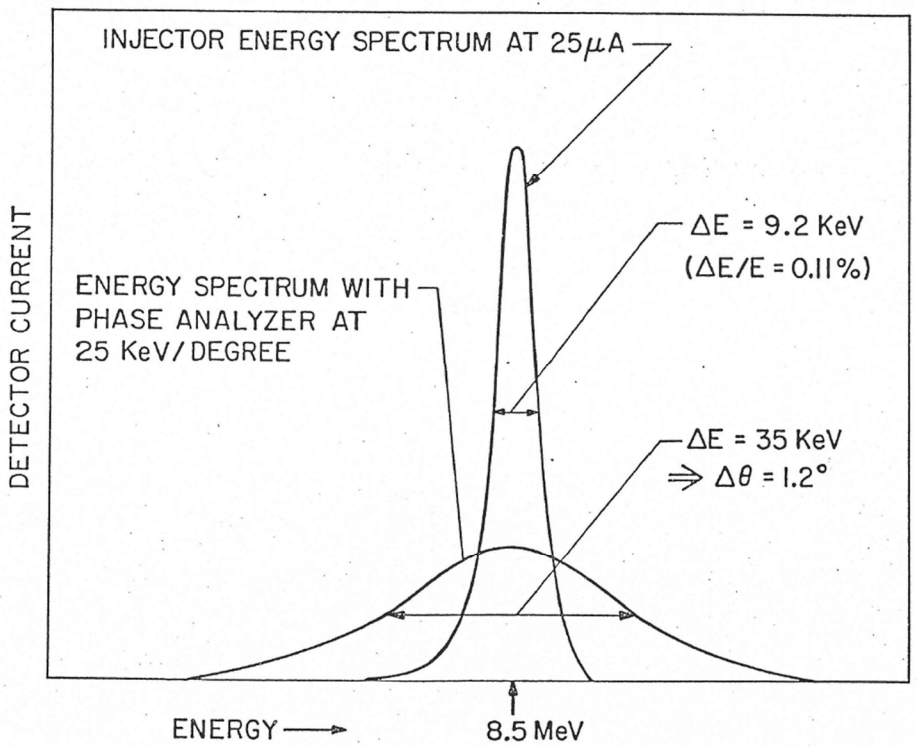

TABLE I. Measured performance parameters for the injector system at a beam current of 25 μA.

100-keV injection emittance	
$\Delta\theta\Delta E$ (90% of beam)	5π keV deg
$\Delta r\Delta\alpha$ (90% of beam)	5π mm mrad
Injector emittance at 8.5 MeV	
$\Delta\theta\Delta E$ (FWHM × FWHM)	11 keV deg
$\Delta r\Delta\alpha$ (90% of beam)	0.3π mm mrad
ΔE (at minimized energy spread)	3.8 keV
$\Delta\theta$ (at minimized energy spread)	2.8 deg
Output from beam filter (8.5 MeV)	
$\Delta r\Delta\alpha$ (90% of beam)	0.6π mm mrad
ΔE	9.2 keV
$\Delta\theta$	1.2 deg
Energy stability (30 min)	$\pm 3\times 10^{-5}$

Note: At 250 uA the spreads in the phase and energy increased by only 10%.

Appl. Phys. Lett., Vol. 22, No. 11, 1 June 1973

TM_{011} Fields

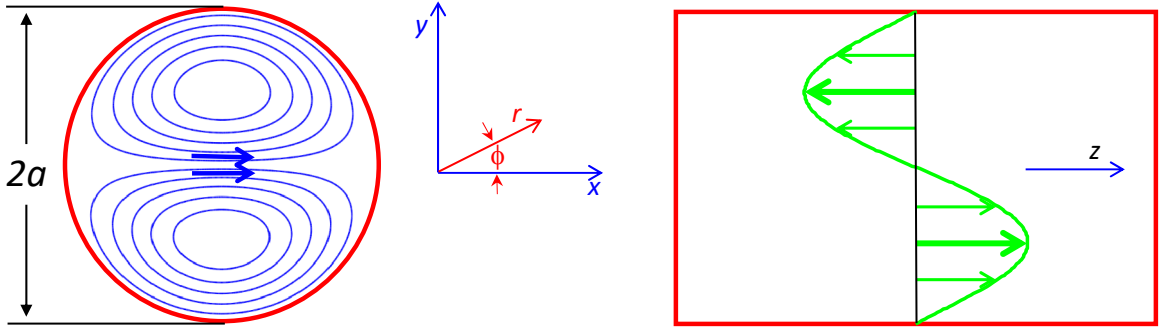

$$B_r = -B_0 \frac{J_1(kr)}{kr}\cos(\phi)\sin(\omega t) \qquad E_z = B_0 c J_1(kr)\sin(\phi)\cos(\omega t)$$

$$B_\phi = B_0 J_1'(kr)\sin(\phi)\sin(\omega t) \qquad k = \frac{\omega}{c} = \frac{2\pi}{\lambda} = \frac{3.833}{a}$$

Near the axis the fields can be approximated as

$B_x = (B_0/2)\sin(\omega t)$ $\qquad$ $E_z = (B_0/2)\,\omega y \cos(\omega t)$

$\omega_{dipole} \sim 1.5\,\omega_{accelerator}$

Remember, there is another TM_{011} mode rotated 90 degrees to this one. Assume that Δf is several bandwidths.

Single Pass Regenerative BBU

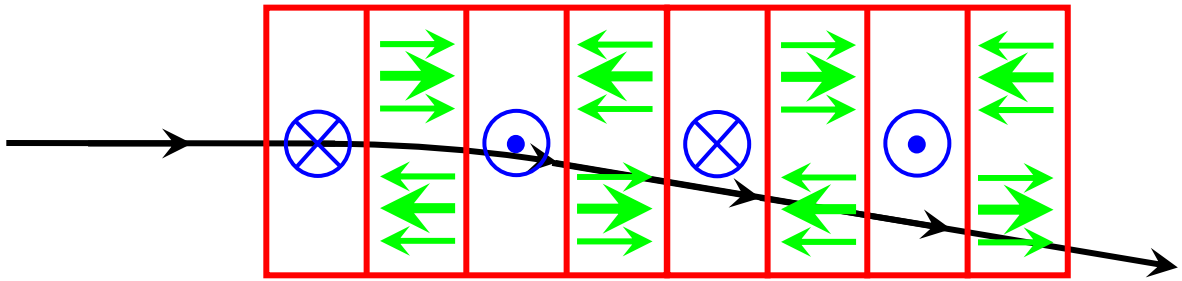

Single Pass Regenerative BBU

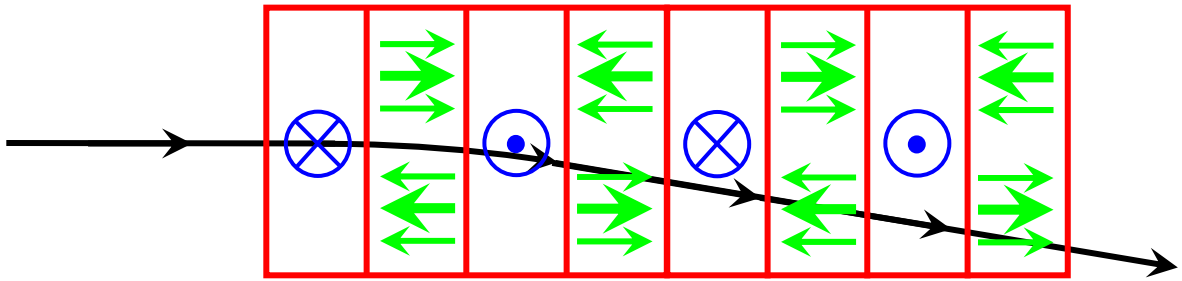

$$I_{threshold} \approx \frac{(\pi/2L)^2 \lambda_d V_{beam}}{(r_d/Q)Q} \qquad r_d = \frac{1}{k^2}\frac{(dE_z/dr)^2}{(P/L)_{cavity}} \approx \frac{100\Omega}{\lambda_{dipole}} Q$$

If L = 1 m, E_{beam}= 10 MeV, $Q_L = 10^9$, and $f_{dipole} \sim 1.5\, f_{acc} = 1.5$ GHz then $I_{threshold} \sim 10$ μa.

BEAM BREAKUP IN A 55-CELL SUPERCONDUCTING ACCELERATOR STRUCTURE*

K. Mittag†, H. A. Schwettman‡ and H. D. Schwarz

Department of Physics and High Energy Physics Laboratory
Stanford University
Stanford, California 94305

Introduction

Longitudinal and transverse beam breakup defines an upper limit to the beam current that can be attained in a linear accelerator.[1,2,3] In a superconducting accelerator (SCA), the problem of regenerative beam breakup is particularly important because the inherent Q-values of the relevant modes are extremely large. On the other hand, the problem of cumulative beam breakup in a SCA is comparable to that in a conventional electron linac.[4] In this paper we describe the regenerative beam breakup characteristics of the 55-cell multiperiodic structure which is the basic unit of the SCA being developed at Stanford.[5] The breakup characteristics of the capture section and the pre-accelerator section have been described previously.[4] In these studies it is demonstrated that the relevant breakup modes can be selectively loaded, and that the starting current for regenerative beam breakup in a SCA can be increased to 500 μA, a value well in excess of the initial design objective of 100 μA.

K. Mittag, H.A. Schwettman, and H.D. Schwartz, IEEE Trans. Nucl. Sci. NS-20, 86 (1973)

TABLE I

BEAM BREAKUP PROPERTIES OF FIRST AND SECOND 55-CELL STRUCTURES

			First structure			Second structure		
Band*	N†	f(MHz)‡	$I_S Q_L$ (10^4A)	Probe**	Q_{ext} (10^7)	$I_S Q_L$ (10^4A)	Probe**	Q_{ext} (10^7)
TM_{01}	42	1297.506	-	-	-	-	-	-
"	43	1297.625	> 770	input	150	> 22,000	input	150
"	44	1297.920	< 0	-	-	< 0	-	-
"	45	1298.353	< 0	input	8	< 0	input	8
"	46	1298.806	< 0	-	-	< 0	-	-
"	47	1299.284	< 0	input	4	< 0	input	4
"	48	1299.745	< 0	-	-	< 0	-	-
"	49	1299.994	-	input	1	-	input	1
"	50	1300.691	> 100	H_θ(S)	80	> 1400	H_θ(S)	80
"	51	1301.000	> 12	input	6	> 160	input	6
"	52	1301.232	> 360	H_θ(S)	470	> 5000	H_θ(S)	470
"	53	1301.495	> 30	input	4	> 400	input	4
"	54	1301.622	< 0	-	-	< 0	-	-
"	55	1301.847	> 13	input	2	> 180	input	2
TE_{11}(1)	1	1470.666	> 300	E_r	70	> 900	H_z(L)	500
" (1)	2	1499.406	> 70	E_r	10	> 210	"	74
" (1)	3	1542.625	> 50	E_r	5	> 150	"	37
" (1)	4	1599.236	9	E_r	5	27	"	37
" (1)	5	1660.242	< 0	-	-	< 0	-	-
TM_{11}	1	1907.660	-	H_z(BP)	77	-	H_z(BP)	77
"	2	1907.466	-	"	21	-	"	21
"	3	1907.103	> 240	"	6.3	> 480	"	6.3
"	4	1906.665	> 160	"	6.5	> 320	"	6.5
"	5	1906.151	> 200	"	10	> 400	"	10
"	6	1905.677	> 240	"	10	> 480	"	10
"	7	1905.213	> 200	"	8	> 400	"	8
"	8	1901.707	> 100	"	14	> 200	"	14
"	9	1900.836	76	"	7	150	"	14
"	10	1899.497	< 0	"	5	< 0	"	5
"	11	1898.105	17	"	4	37	"	4
"	12	1896.455	17	"	5	37	"	5
"	13	1895.128	< 0	"	1.5	< 0	"	1.5
"	14	1894.250	< 0	"	6	< 0	"	6
"	15	1888.787	< 0	"	6	< 0	"	6
"	16	1886.977	> 50	"	3	> 100	"	3

* (1) refers to number of substructure in 6 m structure (See Fig. 1).

† mode number

‡ frequency of only one polarization

** probe which loads mode down to Q_{ext} ; input, H_θ , H_z , E_r label both loading probes and fields to which probes couple; L , S refer to long and short cells, BP to beam pipe (See Fig. 1).

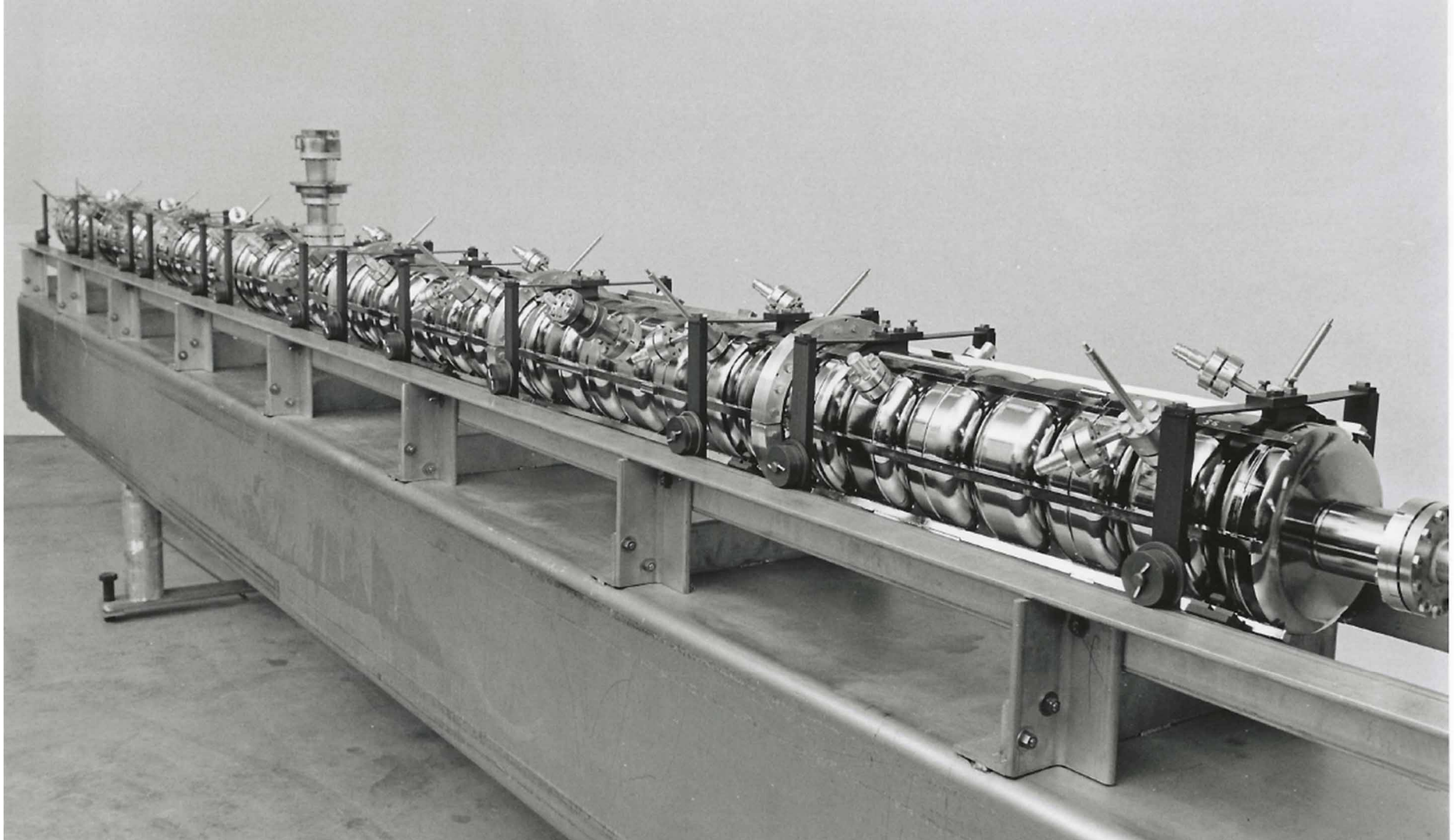

Fission Modes of ^{24}Mg

A. M. Sandorfi

Brookhaven National Laboratory, [a] *Upton, New York 11973, and High-Energy Physics Laboratory Stanford University, Stanford, California 94305*

and

J. R. Calarco, R. E. Rand, and H. A. Schwettman

High-Energy Physics Laboratory, Stanford University, Stanford, California 94305

(Received 27 August 1980)

Coincidence measurements of electrodisintegration products have been used to simultaneously study the $^{12}C + ^{12}C$, $^{16}O + ^{8}Be$, and $^{20}Ne + \alpha$ decay channels of ^{24}Mg. Asymmetric fission into $^{16}O + ^{8}Be$, is concentrated between 18 and 28 MeV in ^{24}Mg and exhibits resonances with cross sections ten times those of symmetric fission. There is little correlation among resonances in the three decay channels. The fission yields are not consistent with statistical decays from giant resonances, and suggest highly clustered states in ^{24}Mg.

Electrons of 26 to 40 MeV from the superconducting accelerator at the Stanford University High-Energy Physics Laboratory were incident on a thin (33- μg/cm^2) ^{24}Mg target at a peak intensity of 220 μA with a duty factor of about 90%.

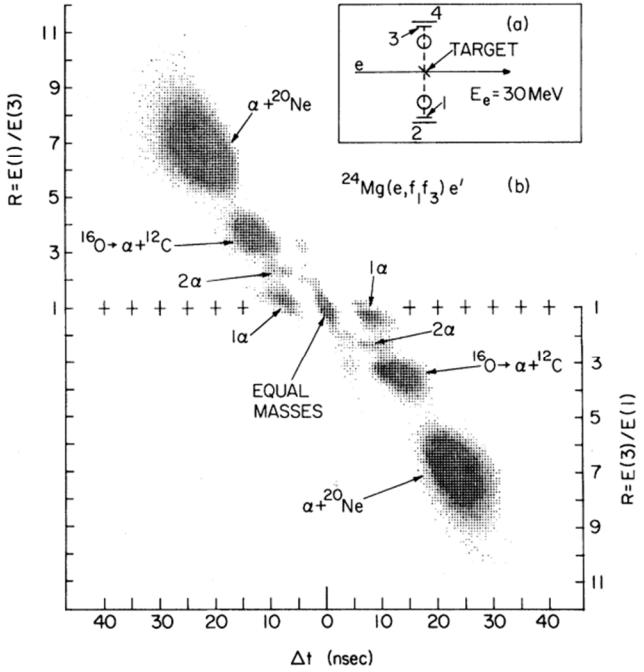

FIG. 1. The coincidence-detection geometry is shown schematically in (a). A density plot of the ratio, formed from the energy of the light fragment over that of the heavy fragment, is shown in (b) as a function of the time difference between their arrival in opposite counters. The origins of the predominant peaks are indicated. Those labeled "2α" ("1α") are from $^{24}Mg \rightarrow ^{16}O + ^{8}Be$ where both (only one) α's from the decaying ^{8}Be are detected.

Phys. Rev. Letts. 45, no. 20 pp. 1615-1616, November 1980

Fission Modes of ^{24}Mg

A. M. Sandorfi

Brookhaven National Laboratory, [a] *Upton, New York 11973, and High-Energy Physics Laboratory Stanford University, Stanford, California 94305*

and

J. R. Calarco, R. E. Rand, and H. A. Schwettman

High-Energy Physics Laboratory, Stanford University, Stanford, California 94305

(Received 27 August 1980)

Coincidence measurements of electrodisintegration products have been used to simultaneously study the $^{12}C + ^{12}C$, $^{16}O + ^{8}Be$, and $^{20}Ne + \alpha$ decay channels of ^{24}Mg. Asymmetric fission into $^{16}O + ^{8}Be$, is concentrated between 18 and 28 MeV in ^{24}Mg and exhibits resonances with cross sections ten times those of symmetric fission. There is little correlation among resonances in the three decay channels. The fission yields are not consistent with statistical decays from giant resonances, and suggest highly clustered states in ^{24}Mg.

Electrons of 26 to 40 MeV from the superconducting accelerator at the Stanford University High-Energy Physics Laboratory were incident on a thin (33- μg/cm^2) ^{24}Mg target at a peak intensity of 220 μA with a duty factor of about 90%.

The experiment required ~150 hours of beam time on the SCA, a factor of 100 less than on a conventional low duty factor linac.

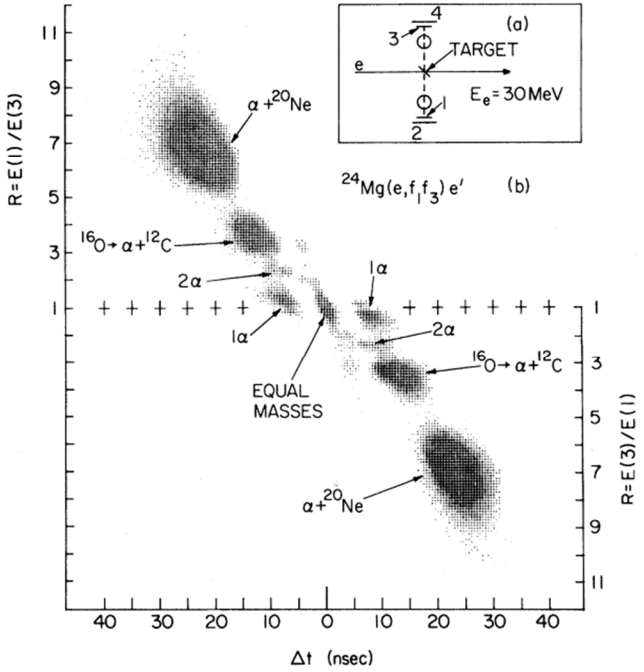

FIG. 1. The coincidence-detection geometry is shown schematically in (a). A density plot of the ratio, formed from the energy of the light fragment over that of the heavy fragment, is shown in (b) as a function of the time difference between their arrival in opposite counters. The origins of the predominant peaks are indicated. Those labeled "2α" ("1α") are from $^{24}Mg \rightarrow ^{16}O + ^{8}Be$ where both (only one) α's from the decaying ^{8}Be are detected.

Phys. Rev. Letts. 45, no. 20 pp. 1615-1616, November 1980

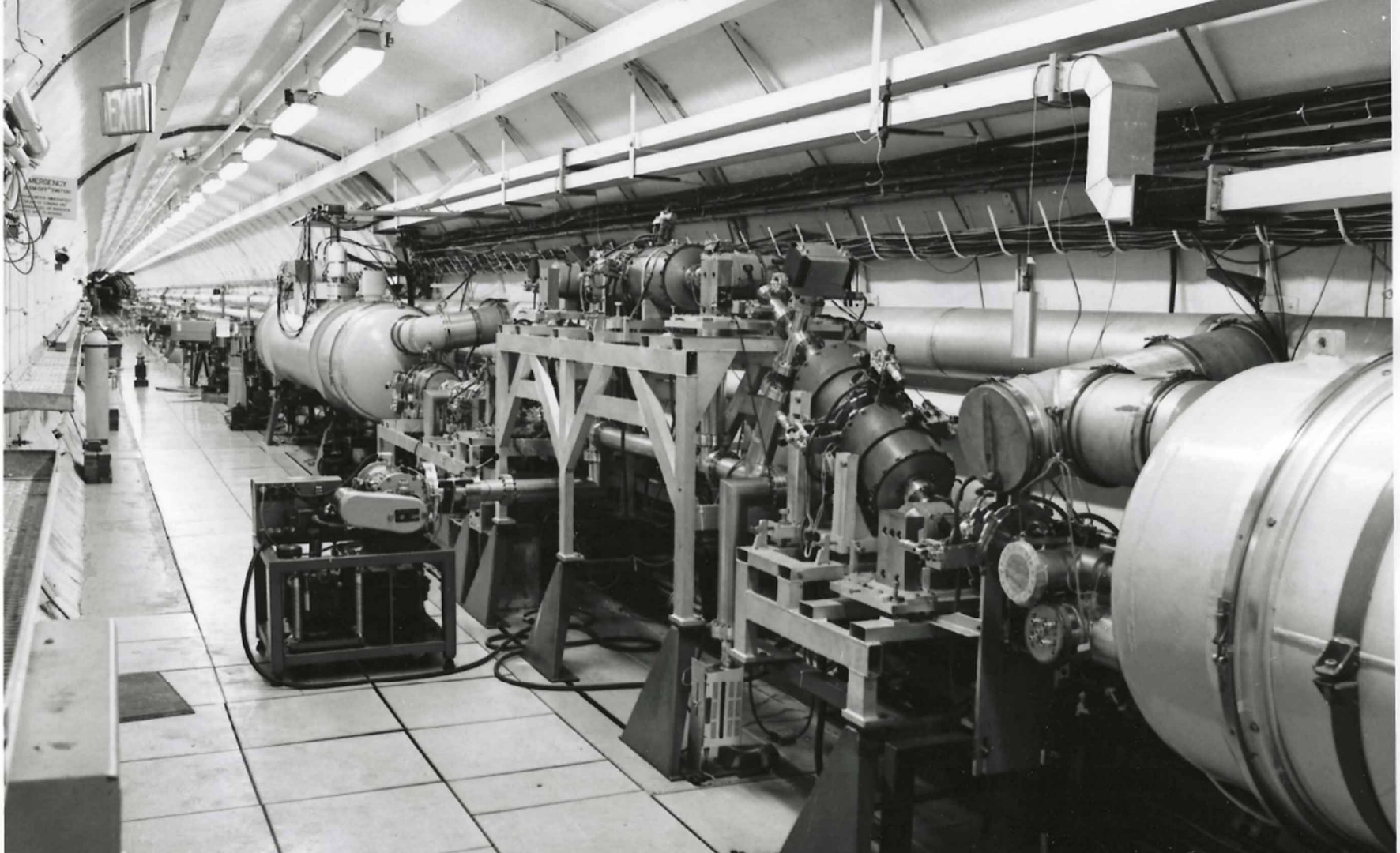
EXIT

Multipass Regenerative BBU

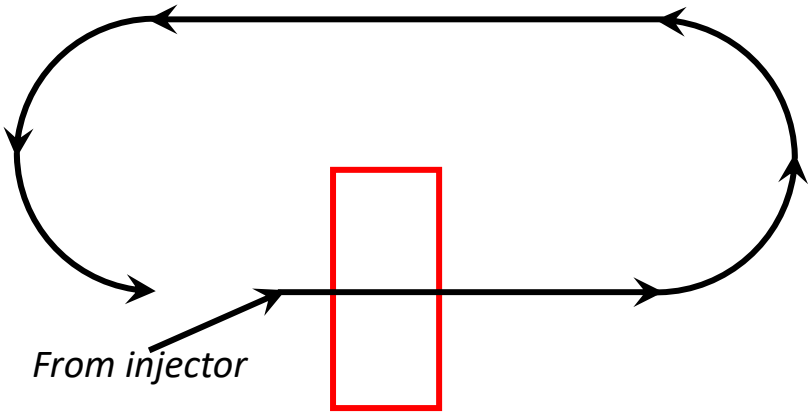

Multipass Regenerative BBU

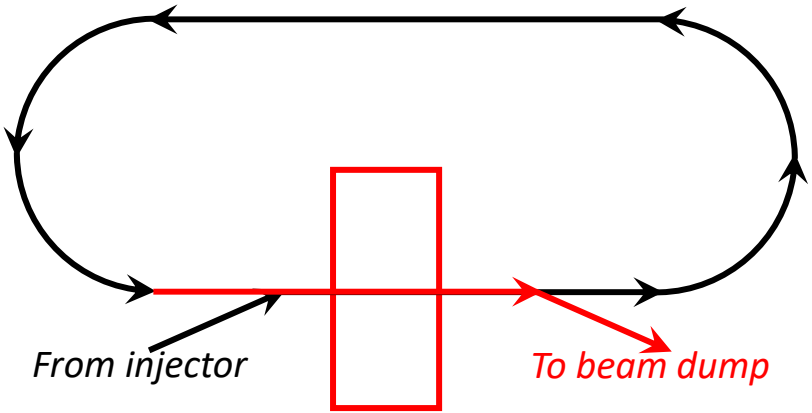

Multipass Regenerative BBU

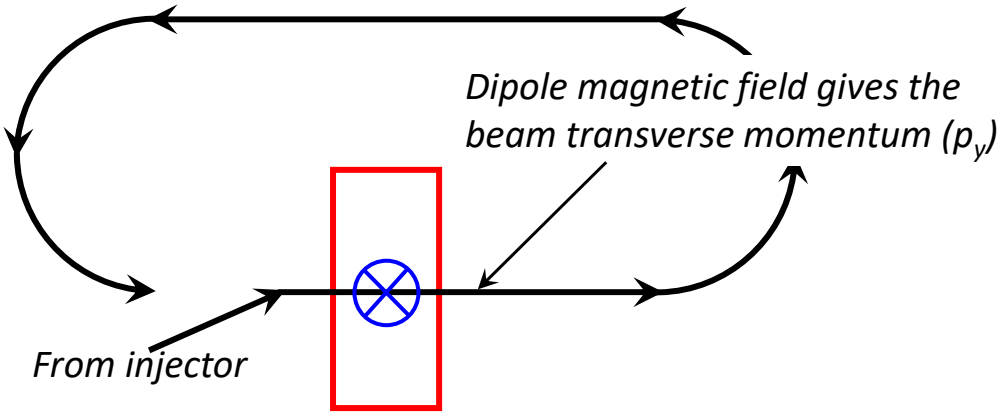

Multipass Regenerative BBU

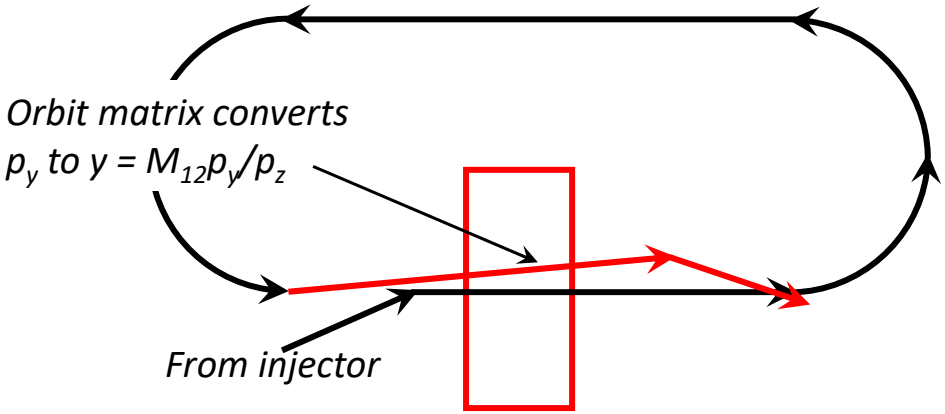

Multipass Regenerative BBU

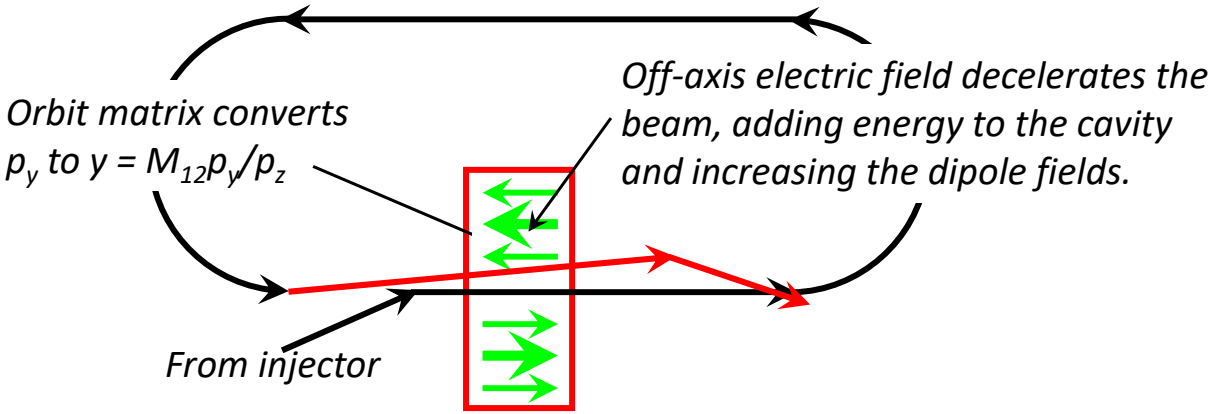

Multipass Regenerative BBU

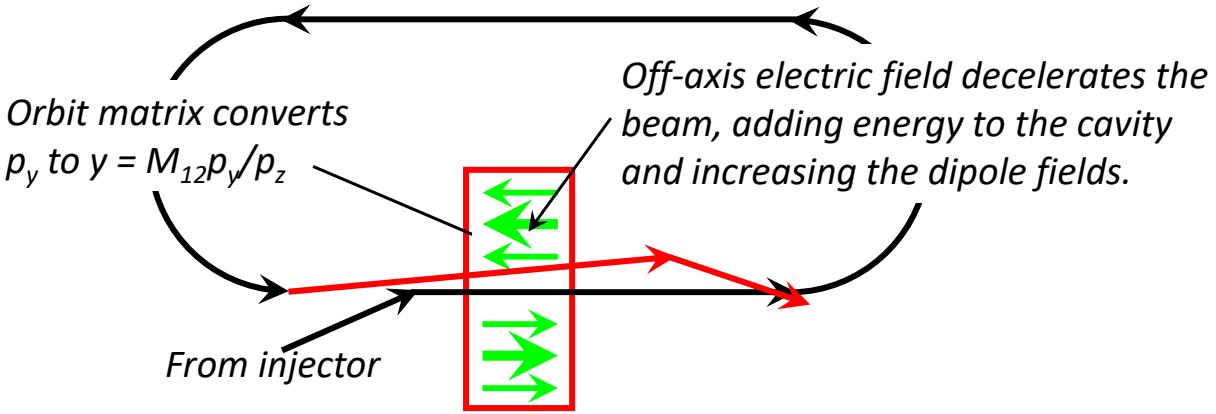

$$I_{threshold} \approx \frac{-\lambda_d V_{beam}}{\pi (R_d/Q) Q \; M_{12} \sin(\omega_d T_r)} \qquad R_d = r_d L_{cavity}$$

recirculation time

With the same cavity as before, and assuming M_{12} = 1 meter, the BBU threshold is now only 1 μa, a factor of 10 lower than single pass breakup.

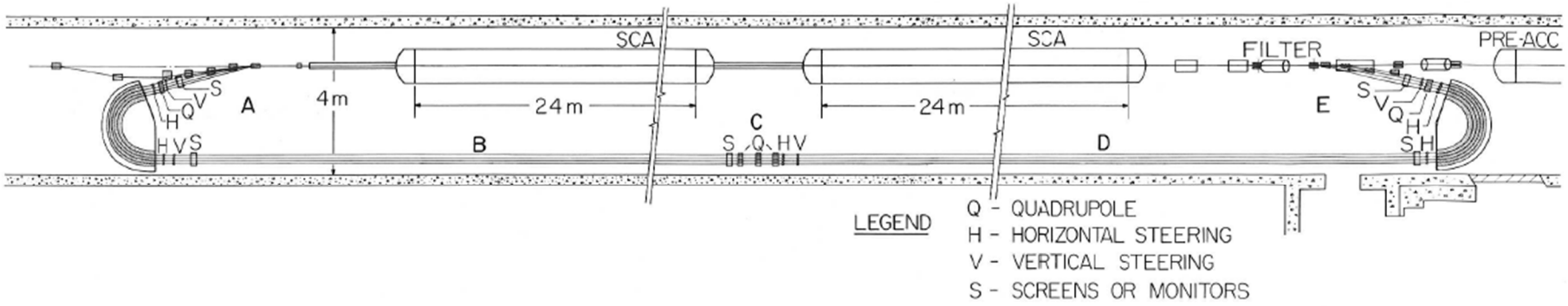

SCHEMATIC LAYOUT OF PROTOTYPE 700 MeV RECYCLOTRON

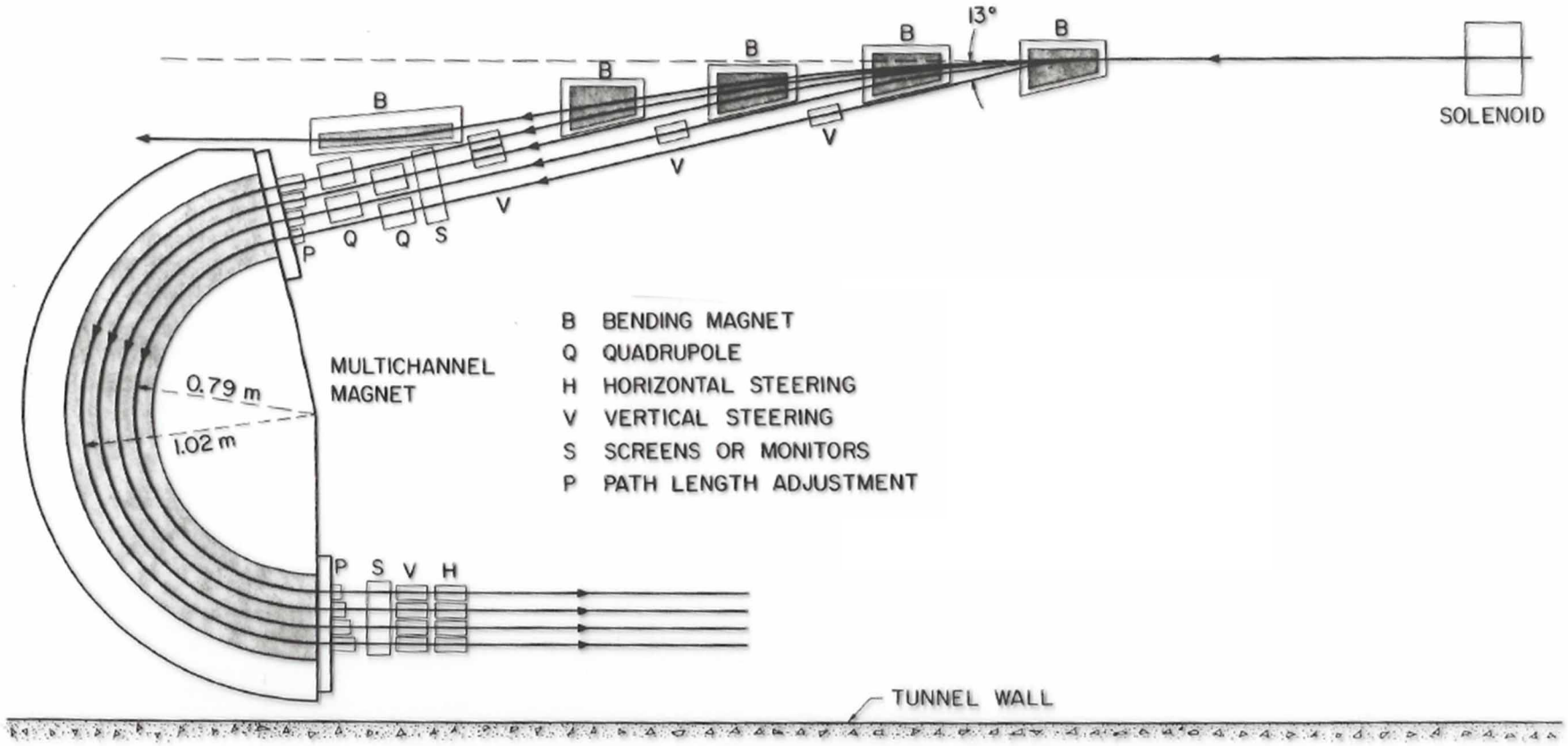

BEAM SEPARATION & MULTICHANNEL MAGNET

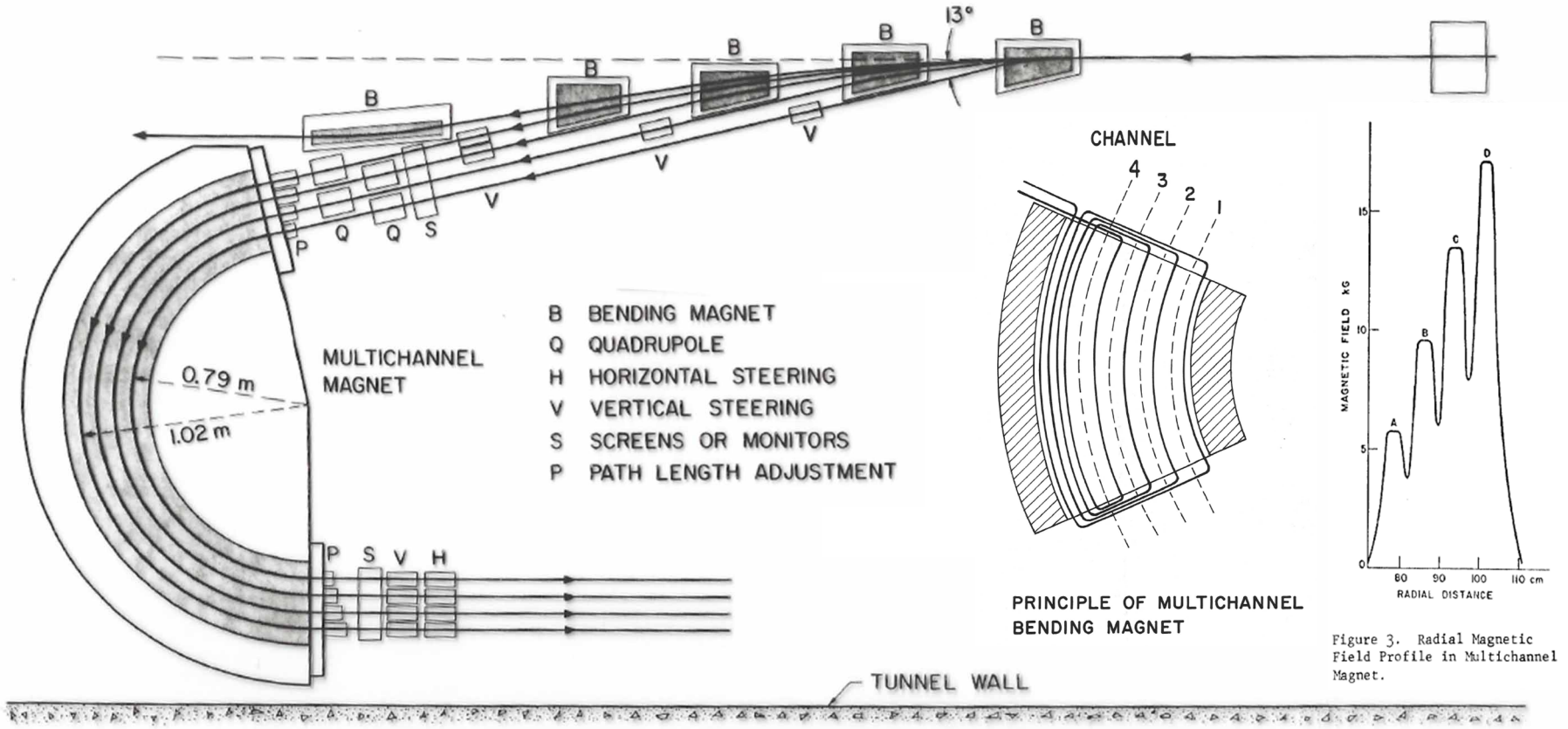

PRINCIPLE OF MULTICHANNEL BENDING MAGNET

Figure 3. Radial Magnetic Field Profile in Multichannel Magnet.

BEAM SEPARATION & MULTICHANNEL MAGNET

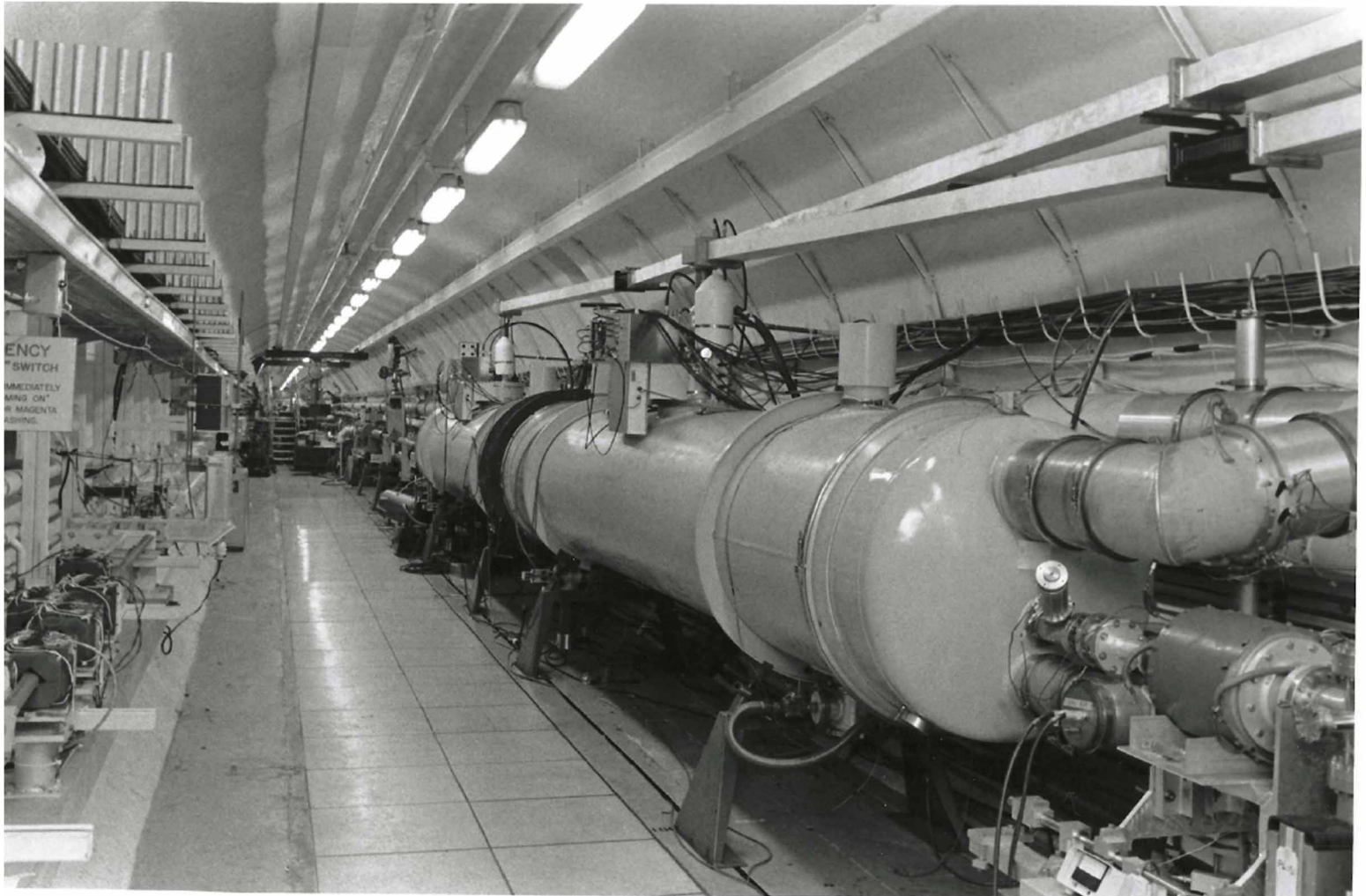
ENCY
SWITCH

DECAY OF GIANT RESONANCES FOLLOWING EXCITATION BY INELASTIC ELECTRON SCATTERING *

J. R. CALARCO
High Energy Physics Laboratory
Stanford University, Stanford, CA 94305 USA

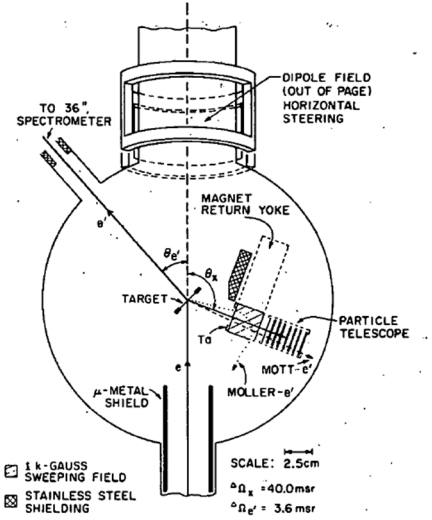

Fig. 1. Chamber geometry for the $^{12}C(e,e'p)$ experiment. The first counter in the telescope is 50 μm thick, the rest are 150 μm.

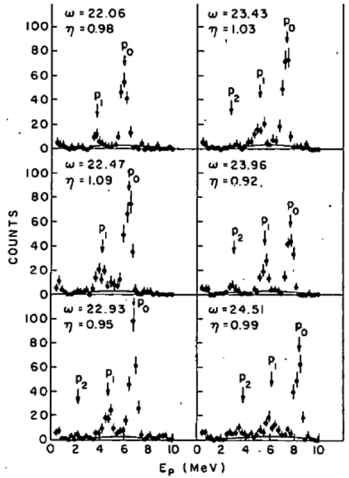

Fig. 3. Typical proton spectra for various values of ω through the region of the GDR with Δω≅150 keV; the GDR peak is near ω=22.9 MeV. The parameter η is the relative efficiency of the e' counters.

Properties of Recirculated Beams

Passes	2	2	3	3	4	4
Energy (MeV)	80	119	117	175	166	232
Duty Factor (%)	75	20	75	20	45	20
Average Current(μA)	50	20	20	13	9	5
Resolution (x 10^{-4})	1.6	1.1	1.1	1.2	1.6	<2

J. R. Calarco, Proc. 1980 RCNP International Symposium on Highly Excited States in Nuclear Reactions, Osaka University, Osaka, Japan, Eds. Ikegami and Muraoka, p. 543, May, 1980;

The Free Electron Laser

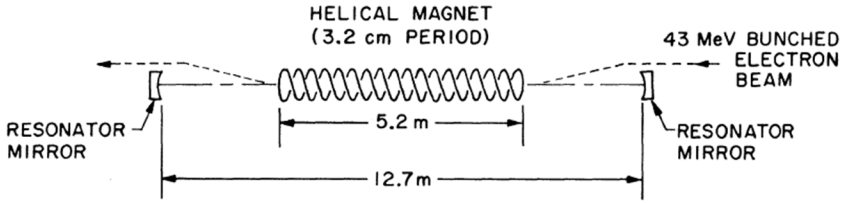

FIG. 1. Schematic diagram of the free-electron laser oscillator. (For more details see Ref. 6.)

TABLE II. Electron beam characteristics.

Energy (Ref. 8)	43.5 MeV
Width (full width at half-maximum):	0.05%
Average current	130 μA
Peak current (Ref. 7)	2.6 A
Emittance (at 43.5 MeV):	0.06 mm mrad

Single 4 ps bunch every 110 RF cycles

Normalized = 5.2 mm mr

TABLE I. Laser characteristics.

Laser characteristics	Above threshold	Below threshold
Wavelength (μm)	3.417	3.407
Width (full width of half-maximum)	0.008	0.031
Average Power (W)	0.36	10^{-8}
Peak power (Ref. 7)	7×10^{3}	10^{-4}
Mirror transmission	1.5%	

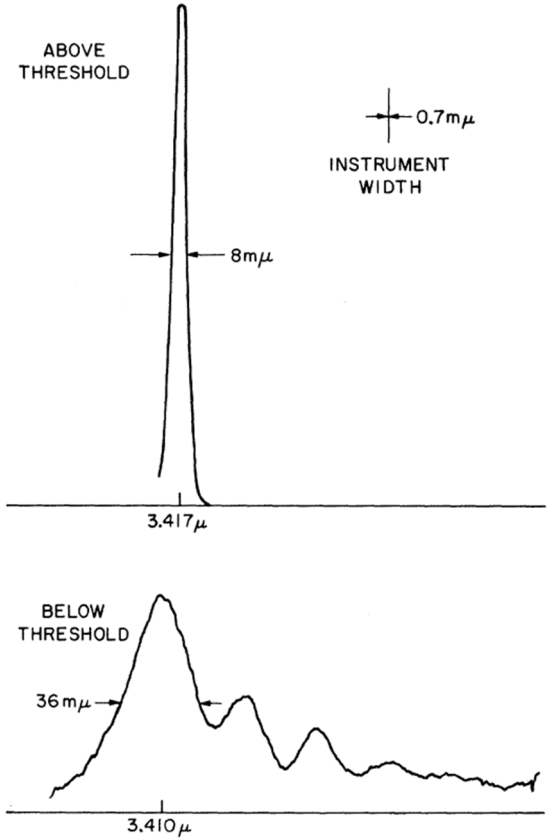

FIG. 2. Emission spectrum of the laser oscillator above threshold (top) and of the spontaneous radiation emitted by the electron beam (bottom).

Phys. Rev. Letts. 38, No. 16, 18 April (1977) pp. 892-894

First demonstration of same-cell energy recovery

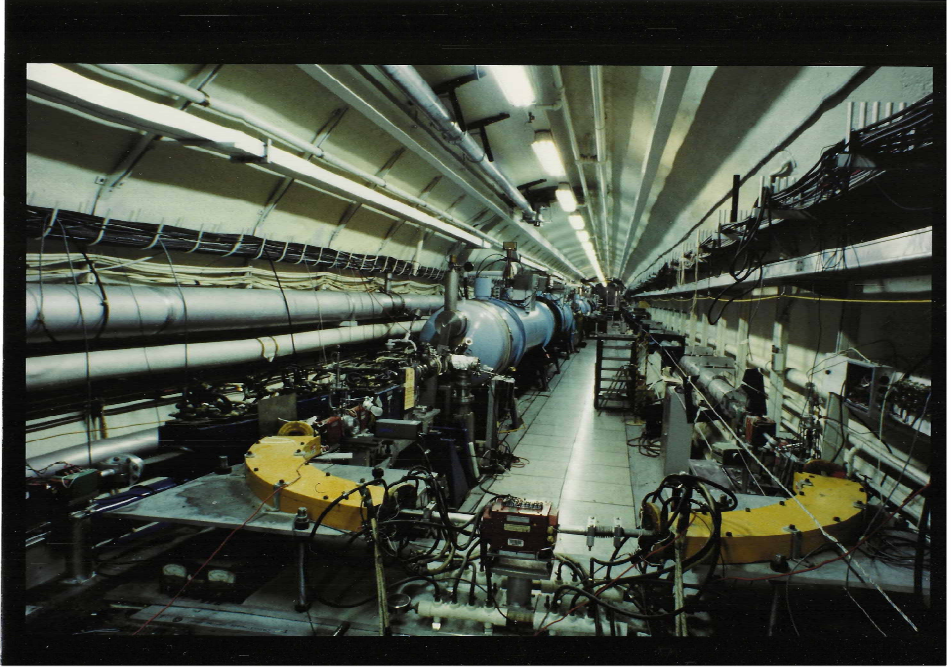

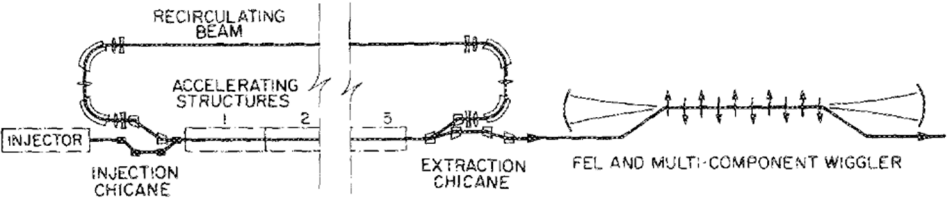

Appl. Phys. Lett. **52** *(19), 9 May 1988*

First demonstration of same-cell energy recovery

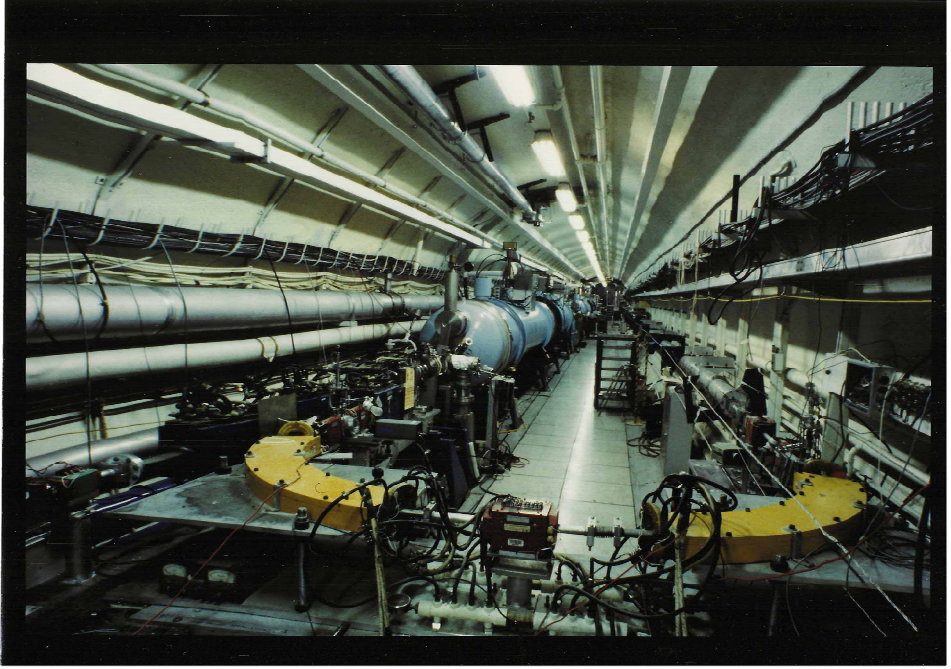

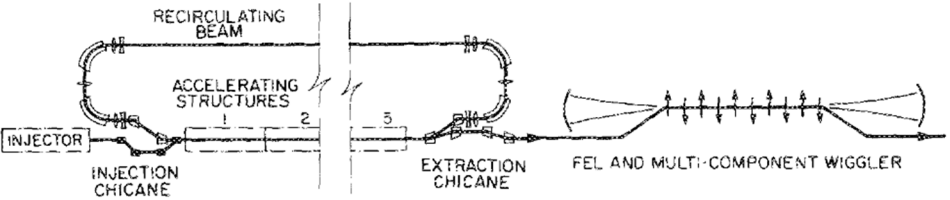

Net rf power required by one of the SCA accelerating structures at constant field level. (a) Large pulse: power required with recirculated beam and system length adjusted to accelerate the recirculated beam. Small pulse: power required with the second pass (recirculated) beam blocked.

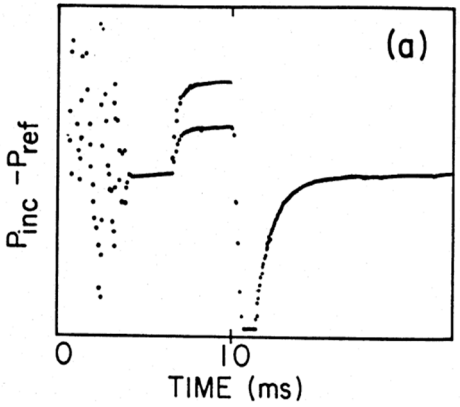

Appl. Phys. Lett. **52** *(19), 9 May 1988*

Nucl. Instr. & Meth. in Physics Research, A259, (1987) pp. 1-7 (North Holland)

First demonstration of same-cell energy recovery

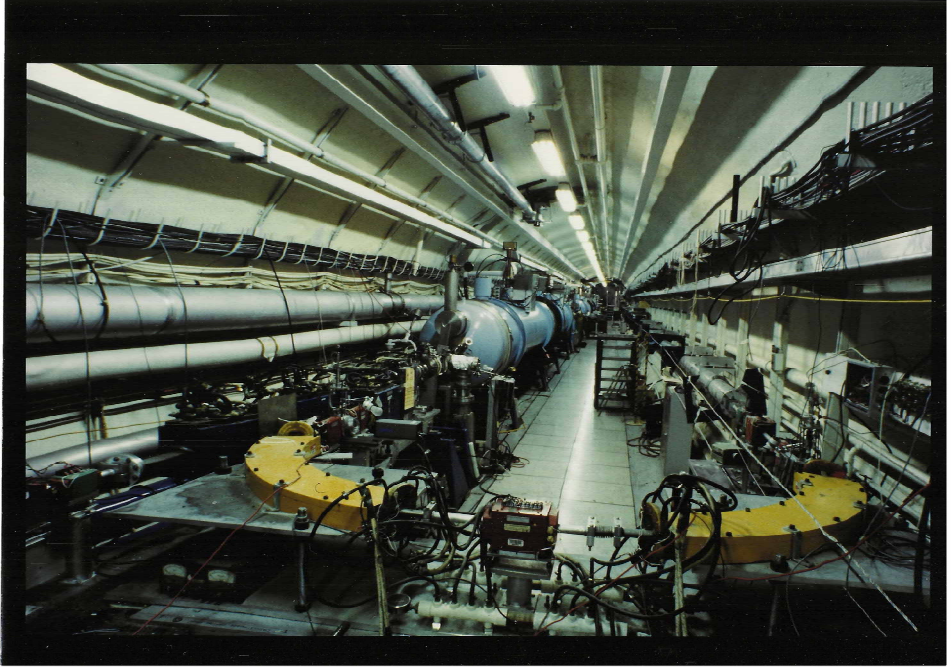

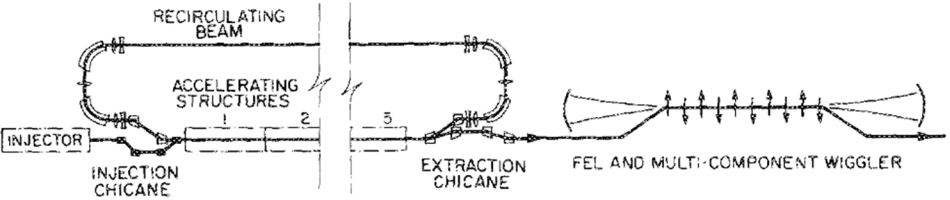

Net rf power required by one of the SCA accelerating structures at constant field level. (a) Large pulse: power required with recirculated beam and system length adjusted to accelerate the recirculated beam. Small pulse: power required with the second pass (recirculated) beam blocked. (b) Small pulse: System length adjusted to decelerate the second pass beam. Large pulse: power required with the second pass (recirculated) beam blocked.

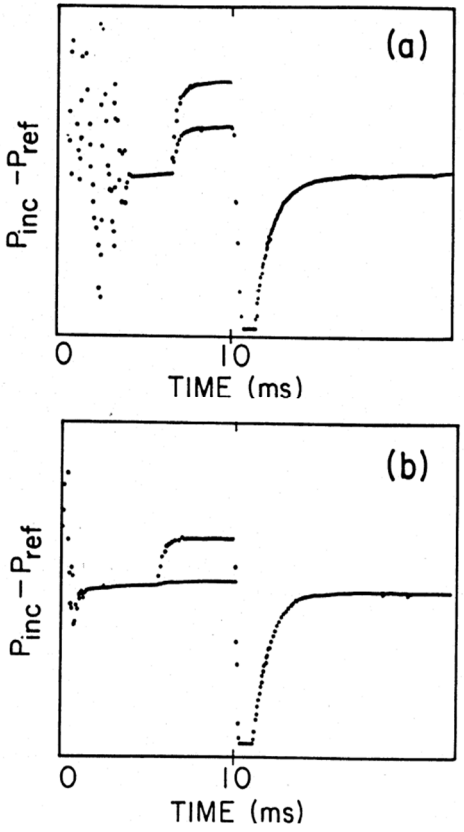

Appl. Phys. Lett. **52** *(19), 9 May 1988*

Nucl. Instr. & Meth. in Physics Research, A259, (1987) pp. 1-7 (North Holland)

Stanford SRF Related Firsts

RF Superconductivity

- *First high Q-values*
- *First high fields*
- *First niobium cavities*

Helium Refrigeration

- *First superfluid helium refrigerator*

Electron Linacs

- *First electron acceleration in a superconducting structure*
- *First feedback control of accelerating fields*
- *First external loading of HOMs*
- *First electron beam recirculation in a linac*
- *First demonstration of same-cell energy recovery*

Free Electron Laser Physics

- *First amplifier experiment*
- *First oscillator experiment*
- *First measurement of optical beam quality*
- *First linac-based lasing in the visible by a FEL*
- *First tapered-undulator oscillator experiment*

The End